CCD APPLICATIONS TO SYNTHETIC APERTURE RADAR

W. Bailey, W. Eversole, J. Holmes,
W. Hoover, J. McGehee, R. Ridings
Texas Instruments Incorporated

W. Arens
Jet Propulsion Laboratory

ABSTRACT. Radar imaging using side-looking synthetic aperture radar techniques is the best known approach for achieving high resolution imagery through atmospheric cloud cover. On-board processing for satellite and small aircraft applications has been prohibitive because of size, weight, and power constraints for digital processors. The powerful computational equivalency of a CCD transversal filter drastically alleviates these constraints, making a CCD image processor feasible for such applications. This paper contains an abbreviated discussion of synthetic aperture principles from which range and azimuth correlators can be defined for a given application. Discussions of CCD constraints, a CCD system design, and a breadboard system are included.

Radar imaging using side-looking synthetic aperture radar (SAR) techniques is the only viable means of achieving high-resolution imagery through atmospheric cloud covers. However, if the radar echo data are not processed into images onboard the spacecraft or aircraft, and if multiple looks are required to achieve acceptable quality, potentially large quantities of raw uncorrelated data must be sent to the ground for processing. Conversely, if images are produced onboard, the multiple-look images may be superimposed into single images and conventional data-compression algorithms may be applied to significantly reduce the data volume and rates transmitted to the ground.

During recent years, considerable effort has been devoted to developing onboard digital data processing of the radar echo data. Unfortunately, results to date indicate that the digital data processing required to produce correlated radar images onboard a spacecraft or small aircraft is normally impractical from cost, complexity, power, size, and weight standpoints. Since only limited compression by means of presumming and time expansion can be accomplished with the uncorrelated radar echo data, proposed radar mission requirements to date have implied the need for reliable high-speed and high-capacity tape recorders for storage, and have imposed potentially severe requirements upon the telecommunications link and ground data handling capabilities.

The discovery of the CCD transversal filter concept[1] has greatly simplified the complicated digital implementation of convolution. A CCD transversal filter of length N bits provides N bits of analog storage while performing N analog signal by weighting coefficient multiplications each clock period. By resolving the SAR processor into a range chirp correlator followed by an azimuth chirp correlator, a considerable reduction in on-board hardware is achievable.[2]

PRINCIPLES OF SYNTHETIC APERTURE RADAR

Generally speaking, when an image of some physical characteristics is needed, the resolution in the two orthogonal directions should be approximately equivalent. This presents a problem to conventional radar sets which could be used to produce an image of the radar cross section of a section of terrain. The resolution of the conventional radar in the radial direction depends directly on signal bandwidth. Pulse-compression techniques permit signal bandwidth to be expanded with negligible sensitivity loss so that adequate range resolution may be realized for many imaging applications.

Azimuth resolution is a more difficult matter, however. Conventional radar azimuth resolution depends ultimately upon the antenna beamwidth.[3] The antenna beamwidth is reduced by increasing the size of the aperture, increasing the carrier frequency, or both. For long-range imaging, however, this approach cannot provide an azimuth resolution which is comparable to the range resolution that can be realized easily with modern pulse-compression techniques.

The solution to this dilemma is provided by synthetic aperture radars (SARs) in which data processing capability is traded for aperture size. In principle, there is no difference between:

An extremely large real antenna, and

A small real antenna that successively occupies all the positions that would be occupied simultaneously by the large real antenna, provided

The data that are successively collected by the small antenna are properly stored and subsequently combined in a simulation of the large real antenna.

Assuming this condition is satisfied, it is possible for a small antenna to move past a scene and record echo data to permit comparable range and azimuth resolution to be realized in an image of the scene after the recorded data have been properly processed.

RANGE PROCESSING

Linear FM chirp pulse compression is an example of spread spectrum techniques which have the properties that probability of detection and resolution are essentially independent quantities. The amount of energy which the transmitter puts into the pulse determines the probability of detection independently of signal bandwidth, assuming a matched-filter receiver. The signal bandwidth is the major factor which determines range resolution.

The principal signal parameter of interest is the RF signal chirp bandwidth, Δf. This parameter defines the compressed pulsewidth. Table 1 shows the compressed pulsewidth for three different weighting functions for the matched filter.

Table 1 shows that, in general, the 3-dB compressed pulsewidth is given by a constant divided by the signal chirp bandwidth, where the constant depends on the type of weighting used, if any, to reduce the range sidelobe level. Resolution is defined as the separation which must exist between two equally strong targets in order for their individual compressed pulse responses to intersect 3 dB below their peak response level. The compressed pulsewidth expressions in Table 1 also give the range resolution for an imaging system in the special case where the radar lies in the plane of the scene being imaged. Actually, the radar will be located above the plane being mapped. This means that the compressed pulsewidth expression of Table 1 must be projected into the plane of the scene in order to obtain the effective range resolution appropriate to the scene.

Table 1. Dependence of Compressed Pulsewidth on Type of Weighting[4]

TYPE OF WEIGHTING	COMPRESSED PULSEWIDTH (MEASURED AT 3-dB POINTS)
Gaussian envelope (−40-dB time sidelobes)	$\frac{1.5}{\Delta f}$
Rectangular envelope (−13.5-dB time sidelobes)	$\frac{0.9}{\Delta f}$
Hamming weighting (−42.8-dB time sidelobes)	$\frac{1.3}{\Delta f}$

Figure 1 shows that the slant range resolution is $c\tau_c/2$ where c is the speed of light and τ_c is the compressed pulsewidth measured at the 3-dB points. Consequently, the range resolution in the plane of the scene is $c\tau_c/2 \sin\theta$ which reduces to

$$\delta_R = \frac{c\tau_c}{2 \sin\theta} = \frac{0.45\ c}{\Delta f \sin\theta} \tag{1}$$

for the case of unweighted linear FM from Table 1. The range correlator's time-bandwidth (TW) product can be defined for a given range resolution and look angle (or chirp bandwidth) and transmitted pulsewidth, T_p, as

$$TW_R = \frac{0.45\ c\ T_p}{\delta_R \sin\theta} \tag{2}$$

AZIMUTH PROCESSING

The basic parameters relating to SAR geometrical relationships are shown in Figures 2 and 3. It is convenient in Figure 3 to think of a stationary radar with target motion being a straight line, as shown. Using conventional terminology, time t is zero when the target is at the point of closest approach. This minimum range value is called R_o.

Data are assumed to be available from the time that the target enters the 3-dB beamwidth point of the real aperture until it leaves the 3-dB beamwidth point on the other side.

At time t, the target is seen in Figure 3 to be displaced a distance Vt from the point of closest approach. The range as a function of time is given by

$$R(t) = (R_o^2 + V^2 t^2)^{1/2} \tag{3}$$

From geometrical considerations, the Doppler frequency can be found as a function of time to be

$$f_D(t) = \frac{-2V^2 t}{\lambda R(t)} \tag{4}$$

where λ is the radar carrier wavelength.

For most cases of interest, the distance Vt in Figure 3 is much less than R_o, so that

$$R(t) \cong R_o \tag{5}$$

The Doppler expression in Equation 4 is approximated by

$$f_D(t) \cong \frac{-2V^2 t}{\lambda R_o} \tag{6}$$

which shows the linear FM chirp characteristic of the Doppler shift between the transmitted and received pulse as a function of the relative position of a point reflector.

The major conceptual difference between the azimuth and range chirp signal is in the signal duration. The range chirp pulse has a rather well-defined start and stop duration. The azimuth chirp modulation has no such well-defined time epoch. The phase of this modulation is determined by the geometrical parameters, but the amplitude is determined by the antenna pattern. As a result, there is the arbitrary matter of azimuth signal duration.

As a practical matter, the effective azimuth signal duration is defined by the signal processor. The charge coupled device

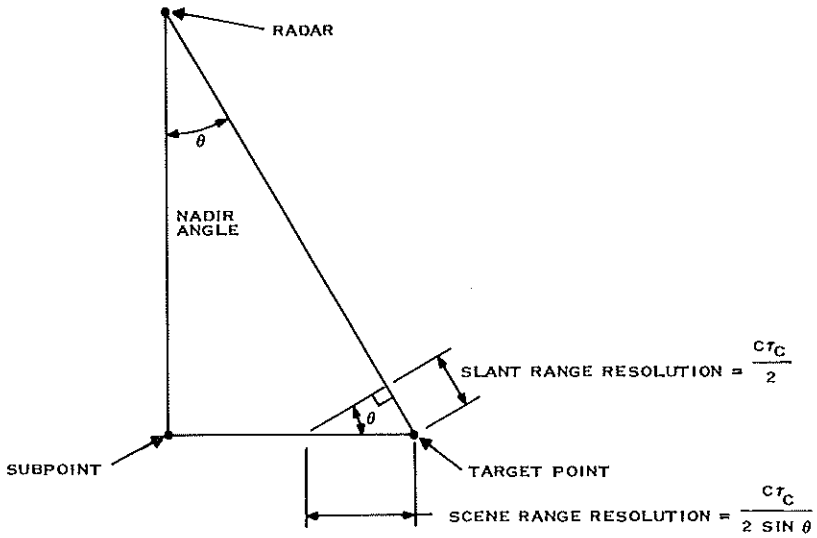

191627

Figure 1. Range Resolution Dependence on Compressed Pulsewidth and Look Angle

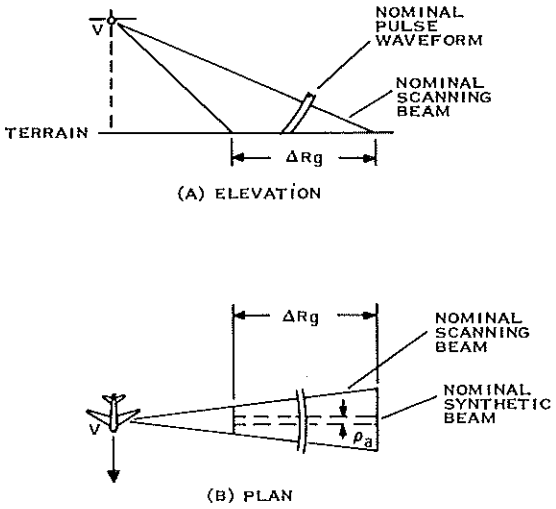

191628

Figure 2. Typical Geometry of Synthetic Aperture Radar System

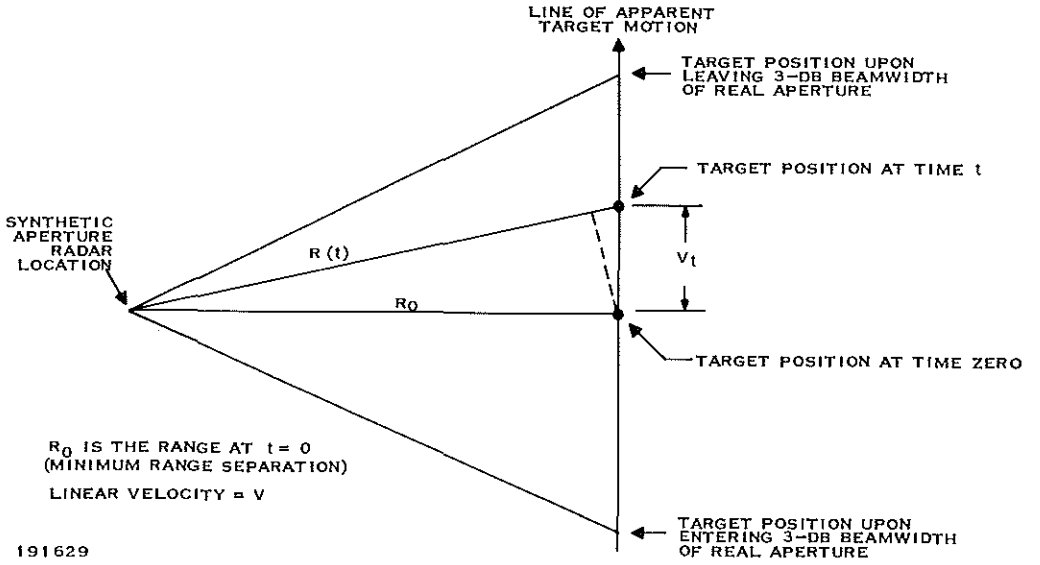

Figure 3. Basic SAR Azimuth Geometry

(CCD) processor functionally contains many azimuth correlation filters which are analogous to the range correlation filters. The azimuth Doppler modulation defined by Equation (6) is assumed to be the signal input to an azimuth correlation filter. The difference is that an azimuth correlation filter needs to process only those signals which correspond to reflectors at the same range. This requires that the echo pulse be divided into range bins following range compression with distinct azimuth correlation filtering provided for each range bin.

The relationships in Table 1 also hold for azimuth compressed pulsewidth. Assuming an unweighted filter, the compressed pulsewidth at the output of the azimuth correlation filter is

$$\tau_c = \frac{0.9}{\Delta f_{AZ}} = \frac{0.45\lambda R_o}{V^2 T_{AZ}} \qquad (7)$$

CCD CONSTRAINTS

The above described resolution constraints as well as other radar system constraints provide physical guidelines for the system design. However, a number of CCD operational constraints[5] which include data rates, charge transfer efficiency, leakage current, and device size are also key factors in determination of the system design.

Equation (1) indicates that chirp bandwidths of approximately 10 MHz may be expected for range resolution in the 10- to 50-meter category. Processing at the Nyquist rate for such a chirp waveform with CCDs represents a difficult implementation task due to feedthrough and bandwidth problems, potentially severe clock power requirements, and possible charge transfer efficiency problems. Since the modular concept allows each module to process on the order of 200 range cells, it becomes possible to sample the radar video at a high rate during a small time window corresponding to the module's swath width once each PRI. The number of samples to be stored is the number of samples required to cover the swath plus the number of bits in the range correlator. While the input sampling rate is constrained by Nyquist considerations, the output data rate is constrained by the PRI making time expansion of the video possible in order to reduce the processor module's data rate. The use of low pass recursive presum filtering techniques offers further reduction in the data rate and storage requirements. Following time expansion, the samples are clocked into a complex (I and Q) CCD correlator which performs pulse compression on the received chirp radar returns at a clock rate of 1 MHz or less, avoiding the high-frequency video design requirements and possible high-frequency CTE degradation.

Charge transfer efficiency requirements for this SAR design does not represent a serious problem with the present state of the art. Table 2 indicates the effects of CTE upon range resolution for a Hamming apodized, Nyquist sampled correlator having a TW product of 62. The relative resolution is the ratio of the −3-dB correlation pulsewidths for each CTE to the ideal transfer case. CTEs greater than 0.999 appear to result in minimal resolution degradation. In multiple-look SAR systems requiring cascaded azimuth correlators, CTE requirements are more demanding than indicated in Table 2. Also, leakage current problems appear to be more severe.

Equation (8) indicates the inverse relationship between azimuth correlation time and resolution. Since integrated leakage current can ultimately fill the potential well containing the charge signal sample, leakage current will ultimately limit azimuth resolution.[6]

Table 2. Resolution and Amplitude Degradation as a Function of CTE for a Correlator Having a TW Product of 62

CTE	RELATIVE RESOLUTION	RELATIVE ATTENUATION (dB)
1.0	1.000	0
0.9999	1.005	−0.068
0.999	1.047	−0.673
0.99	1.679	−5.757

The azimuth resolution distance is obtained by multiplying this compressed pulsewidth by velocity to obtain

$$\delta_{AZ} = V\tau_c = \frac{0.45\lambda R_o}{VT_{AZ}} \tag{8}$$

for an ideal processor which is unweighted. Amplitude weighting has the effect of broadening the compressed pulsewidth and reducing the sidelobe level. Equations (7) and (8) define the azimuth correlator's TW product for the unweighted case as

$$TW_{AZ} = \frac{0.405\lambda R_o}{\delta_{AZ}^{\,2}} \tag{9}$$

Equation (8) shows that the azimuth resolution can be improved only by increasing the azimuth correlation time, assuming that the geometrical parameters R_o, λ, and V are fixed.

The amount of integrated leakage current contributed to the charge packet at the k^{th} bit location is

$$\Delta Q_{KL} = \int_o^{Tc} J_{KL}\, A\, dt \tag{10}$$

where

J_{KL} = leakage current density

A = bit area

T_c = clock period.

The effect of the leakage current upon the transversal filter's output is seen from the relationship

$$V_{out} \propto \sum h_K Q_K = \sum h_K (Q_{KS} + Q_{KL})$$

$$= \sum h_K Q_{KS} + \sum h_K Q_{KL} \tag{11}$$

$$= \sum h_K Q_{KS} + \text{constant}$$

where Q_{KS} is the signal charge and Q_{KL} is the integrated leakage current present in the k^{th} storage location.

The integrated leakage current at the k^{th} location for a constant clocking rate and temperature is a constant which, when multiplied by the weighting coefficient h_K (a constant) gives a constant. Therefore, the integrated leakage current has a first order effect of an output dc level shift.

Since the total integrated leakage current (Q_{KL}) increases linearly (excluding statistical variations) down the transversal filter, the transversal filter is much more tolerant of leakage current than other CCD device types.

Satisfactory correlator operation can be achieved with integrated leakage currents on the order of ten percent of a full well at the CCD output. Azimuth correlation times of 0.5 second have been achieved at room temperature. Longer correlation times, multiple looks in azimuth, or higher temperature environments may require improved leakage current characteristics or the use of thermoelectric coolers.

SYSTEM CONFIGURATION

The system represented in Figure 4 has been developed to avoid many of the operational difficulties experienced with CCDs. The input sampler stores samples of the appropriate swath width at the high frequency rate required by range resolution and Nyquist considerations. The sampler's output rate is constrained by the number of samples stored and the PRI. The optional presum filter permits reduction in the length of the azimuth correlators and in the data rate.

Following time expansion, the samples are clocked into a complex (I and Q) CCD correlator which performs range pulse compression on the received chirp radar returns. The output signal sequence is a complex (I and Q) representation of radar cross section (amplitude) versus range (time). By range sorting this output, it may be observed that returns in a given range bin on sequential PRIs are samples of the Doppler chirp from a target. Therefore, pulse compression in azimuth may be achieved by functionally feeding the range sorted samples into a bank of azimuth chirp correlators each PRI. The pulse compression performed by the correlators is responsible for the Doppler beam sharpening attendant with the SAR azimuth resolution improvement. The azimuth correlators also subtly perform the analog storage of sequential radar returns as required by basic SAR principles.

The I and Q outputs of the azimuth correlator bank are then multiplexed, squared, and summed to form a video line in the range direction. An additional line corresponding to subsequent azimuth positions occurs each PRI.

The system can easily be configured into a modular concept where modules may be stacked to provide additional coverage in the range dimension. This also facilitates the use of range correlators having different chirp slopes to avoid defocusing problems present in some applications. An estimate for such a module covering a 10-km swath width with 50-m resolution

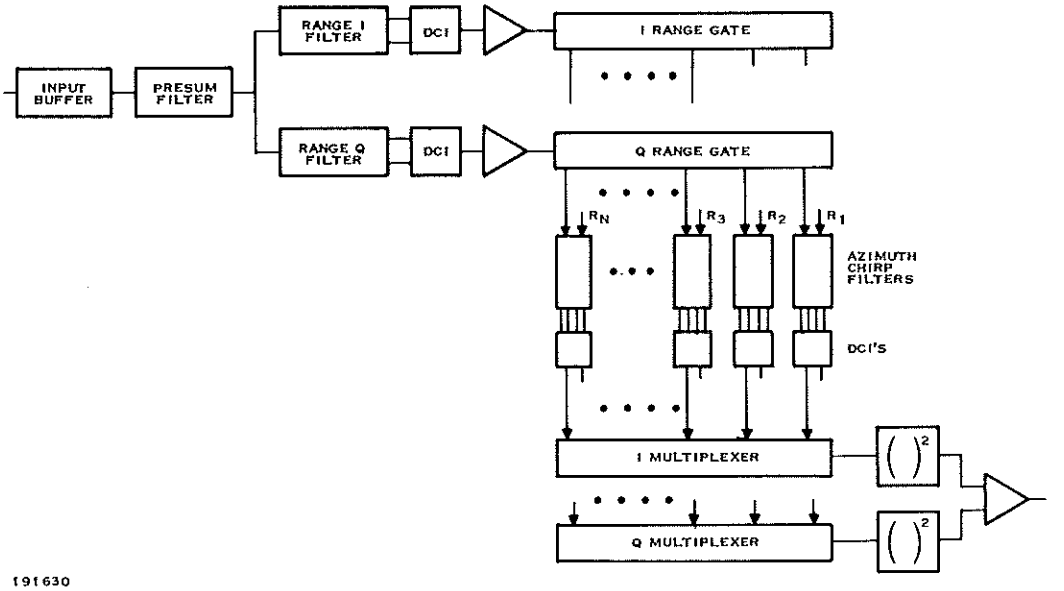

Figure 4. Synthetic Aperture Radar Functional Diagram

from an altitude of 800 km, indicates the following parameters are achievable with such a processor.

Weight	≤7 lb
Size	≤150 in³
Power	≤7 watts

BREADBOARD AND TEST SYSTEM

A simplified version of the system shown in Figure 4 has been constructed to demonstrate the processor concept. A single azimuth correlator was constructed which is sequentially stepped through the 200 range bins with a minicomputer in order to minimize hardware construction. The radar/platform parameters for this breadboard system shown in Table 3 are relatively representative of an aircraft radar environment. Range and azimuth correlation is accomplished with Hamming weighted linear FM complex filter pairs having TW products of 62 and 16, respectively. Range and azimuth correlation times are 0.47 ms and 0.5 s, respectively.

In order to form a 200- by 200-element picture with this breadboard, a TI 960A computer with a 28K memory used in conjunction with a 1,100,000 word disk memory and a nine-track, 800-BPI magnetic tape unit were used. The simulated radar echo pulses were transferred from the tape to the disk. The simulated radar bursts correspond to radar returns from a swath of interest at sequential azimuthal locations. By re-circulating this sequence of bursts to the breadboard while sliding the azimuth read-in time window across the swath time, a complete picture can be processed an azimuth column at a time. To reconstruct the picture, the output of the azimuth correlator is digitized and stored in memory. The memory can then be used much as a scan converter to refresh a CRT display. Full implementation of the azimuth correlator bank would provide real time processing.

Figure 5(A) indicates a portion of the uncompressed video signal corresponding to 48 point targets arranged in four rows in the range dimension. The point targets have a random signal phase and increase in intensity along the azimuth direction in 2-, 4-, 6-, and 8-percent increments for each of the range rows. The compressed point target image is shown in Figure 5(B).

Table 3. Breadboard Radar/Platform Parameters

Altitude	5.0 km
Slant Range	10.0 km
Nadir angle	60.0 degrees
Velocity	320.0 m/s
Wavelength	32.0 cm
Frequency	936.84 MHz
Transmitted pulse duration	3.58 μs
Transmitted signal bandwidth	17.32 MHz
Echo pulse duration	15.12 μs
Slant-range resolution	8.66 m
Along-track ground resolution	10.0 m
Cross-track ground resolution	10.0 m

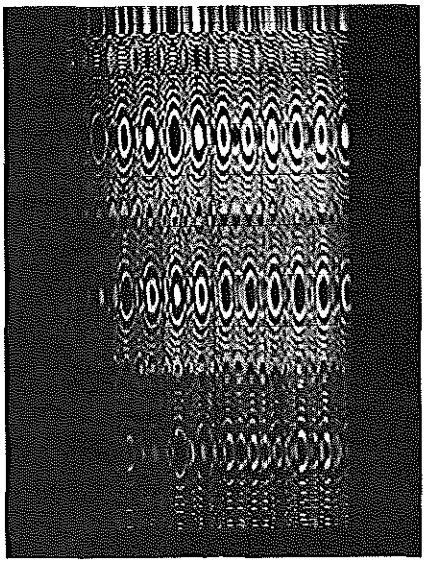

RANGE

AZIMUTH

(A) UNCOMPRESSED VIDEO

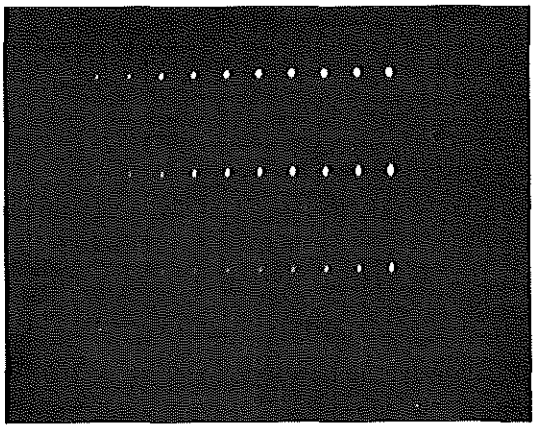

INTENSITY STEPS

8%

6%

4%

2%

RANGE

AZIMUTH

(B) PROCESSED PICTURE

191631

Figure 5. Image Processor Response to Varying Intensity Point Targets

ACKNOWLEDGMENTS

The development of the SAR breadboard processor discussed in this paper was sponsored by Cal Tech Jet Propulsion Laboratory (JPL) under Contracts 953954 and 954087. The authors would like to acknowledge Verie Lima, Dennis Buss, and Dennis Young of Texas Instruments and Robert Grey, Rolando Jordan, Richard Mattingly, and Thomas Thompson of JPL for their efforts associated with this work.

REFERENCES

1. D. R. Collins, W. H. Bailey, W. M. Gosney, and D. D.Buss, "Charge Coupled Device Analog Matched Filters," Electronic Letters, 8, June 29, 1972, pp. 328-329.

2. G. T. Coate, excerpt from unidentified report to AFAL.

3. W. M. Brown and L. J. Porcello, "An Introduction to Synthetic Aperture Radar," IEEE Spectrum, September 1969.

4. C. E. Cook and M. Bernfeld, Radar Signals: An Introduction to Theory and Application, Academic Press (New York 1967), p 197.

5. D. D. Buss and W. H. Bailey, "Applications of Charge Transfer Devices to Analog Signal Processing," IEEE, 1974 Intercon Technical P.

6. A. F. Tasch, R. W. Brodersen, D. D. Buss, and R. T. Bate, "Dark Current and Storage Time Considerations in Charge Coupled Devices," Proceedings of CCD Applications Conference, 18-20 September 1973 (San Diego, California), pp. 179-187.